EXTENDED NUMERICAL ANALYSIS FOR THE MAGNETIC NANOFLUID DROPLET HEATING AND VAPORIZATION

César F. C. Cristaldo[1], **cristaldo@lcp.inpe.br**
Andris Bakuzis[2], **bakuzis@if.ufg.br**
A. L. De Bortoli[3], **dbortoli@mat.ufrgs.br**
Fernando F. Fachini, fachini@lcp.inpe.br

[1]Laboratório de Combustão e Propulsão - LCP
Instituto Nacional de Pesquisas Espaciais - INPE
12630-000, Cachoeira Paulista, SP, Brasil

[2]Instituto de Física
Universidade Federal de Goias
74001-970, Goiânia, GO, Brasil

[3]Instituto de Matemática
Universidade Federal do Rio Grande do Sul
91509-900, Porto Alegre, RS, Brasil

Abstract. *A variety of phenomena in combustion are exhibited by the burning of a spherical liquid fuel droplet in an oxidizing atmosphere. Here we consider the heating, vaporizing and burning of a simple droplet constituted by a magnetic nanofluid (ferrofluid) in a high temperature environment. Since the combustion of liquid fuels occurs in the gas phase, the control of the droplet temperature evolution determines the heating and the vaporization processes. Besides the heat flux from the ambient atmosphere to the droplet, an extra heat source is introduced when the droplets are in the presence of an external alternating magnetic field. The interaction between the magnetic field and the dipoles of the magnetic nanoparticles produces a torque rotating the particles to align the dipoles with the magnetic field. The particles rotation is against viscous forces and heat is generated by the friction. The analysis are conveniently organized to show the influence of the magnetic field frequency on the droplet heating and vaporization time.*

Keywords: *Droplet, Nanofluid, Combustion, Hyperthermy*

1. INTRODUCTION

Magnetic fluids (magnetic nanofluids or ferrofluids) are colloidal magnetic systems resulting from the combination of a fluid with nanoparticles uniformly dispersed. Magnetic Nanofluids find a variety of applications in various fields such as packaging, electronic, mechanical engineering, aerospace, bioengineering, and thermal engineering [Xuan, *et al.*, 2007]. The main reason for this interest is the easy control and monitoring systems containing fluids or magnetic particles, the rapid response of these fluids when subjected to the action of a magnetic field.

A fluid with magnetic nanoparticles when exposed to an alternating magnetic field can generate heat due to the rotation of the nanoparticles, produced by the interaction of the external magnetic field with the magnetic dipoles of the nanoparticles, against the liquid viscous forces [Rosesweing, 2002]. Since the diameter of the suspended magnetic particles is usually about 10 nm, these nanoparticles are considered to have a single magnetic moment [Xuan, *et al.*, 2007]. The Brownian motion always leads nanoparticles in random motion [Kac, 1947] causing a misalignment of the magnetic dipoles. The alternating magnetic field will align the magnetic dipole of the nanoparticles, the particle can rotate with the magnetic dipole (Brownian relaxation). When this occurs, the rotation of the nanoparticle causes friction with the surrounding fluid, generating heat.

This process, knowing as hyperthermia, is utilized as a treatment of cancer, where cancer cells with magnetic nanoparticles inside are destroyed by heating when exposed on an alternating magnetic field. We intend to use the hyperthermia in the burning process of droplet fuel to heat the droplet rapidly and consequently increasing the rate of vaporization.

Evaporation of the fuel has a direct effect on the rate of spray combustion because the fuel must be vaporized to react chemically with the oxidizer. Thus, the thermodynamic efficiency of a motor is affected by the rate of evaporation. And furthermore, the evaporation of fuel can have significant effects on emissions of pollutants [Stiesch, 2003]. With that in mind, we explore the idea of including the process of hyperthermia to reduce the time to warm up and increase the rate of vaporization.

Since the nanoparticles distribution inside the droplet is considered uniform, the effect of the magnetic field is also uniform throughout the droplet. Thus, the temperature profile depends only on the time. However, there is a thermal boundary layer close to the droplet surface in which both heat sources (magnetic and thermal) have the same importance

[Sirignano, 1999]. Therefore, in the thermal boundary layer, the temperature changes spatially. To obtain the temperature profile in the thermal boundary layer, the time and the spatial variables must be appropriately rescaled. In previous works [Cristaldo, 2010], the heat flux from the ambient atmosphere to the droplet is prescribed, thus the liquid phase problem becomes decoupled from the gas-phase problem.

The present analysis couples the liquid phase problem with that of the gas phase, so heat flux is found as a part of the solution. Under this condition, the procedure to solve the problem is to prescribe a droplet surface temperature, to find the solution of the problems of the two phases and to compare if the heat flux at the droplet surface satisfies the heat conservation at the interface liquid-gas. In the energy conservation for the liquid phase, the magnetic power source has to be included. This source term is dependent on the frequency of the magnetic field, magnetic power and temperature. The problem is solved numerically by the finite difference method.

2. MODEL FORMULATION

The droplet is assumed to be spherical with radius $a(t)$ at time t, $a_0 = a(0)$ being the initial value, so that it has spherical symmetry in the liquid phase. It is assumed that the density ρ, the specific heat c_l and thermal conductivity of the liquid phase k_l are constant. The dimensionless variables used in this work are defined as:

$$t \equiv t^*/t_c, \quad r \equiv r^*/\bar{a}_0, \quad \theta \equiv T/T_B, \quad a \equiv a^*/a_0^* \tag{1}$$

where $t_c = [a_0^{*2}/(k_g/c_p\rho_\infty)](\rho_l/\rho_\infty)$ is an estimative of the heating time of the droplet, T_B is the boiling temperature and a is the dimensionless radius of the droplet. The dimensionless conservation equations for mass and energy, are given by [Fachini, 2009] as

$$\frac{d}{dt}(a^3) = -3\lambda^* \tag{2}$$

$$\frac{\partial\theta}{\partial t} - \frac{A}{r^2}\frac{\partial\theta}{\partial r}\left(r^2\frac{\partial\theta}{\partial r}\right) = P_m\frac{f^2\tau_m(\theta)}{1+(f\tau_m(\theta))^2} \tag{3}$$

where , $A = c_p k_l/c_l k_g$, $f = 2\pi\bar{f}t_m^*$ is the dimensionless frequency, $\tau_m(\theta)$ the relaxation time, a function of temperature, $\lambda^* = \dot{m}c_p P_m/(4\pi k_\infty a_0)$ is the dimensionless vaporization rate that varies with time and

$$P_m = \frac{\mu_0\chi_0 H_0^2/2}{\rho_l c_l T_B}\frac{t_c}{t_m^*} \tag{4}$$

where μ_0 is the magnetic permeability, χ_0 the magnetic field amplitude and H_0^2 and t_m^* the relaxation time at boiling temperature. P_m represents the ratio of the power magnetic to the thermal power . The model proposed in this paper considers the case $P_m \gg 1$. This means that the power magnetic is much larger than the thermal power due to the heat conduction from the gas phase. An analysis on Eq. (3), for $f \gg 1$ the time scales would be $\tau \sim P_m^{-1}$ and for $f \ll 1$, $\tau \sim f^{-2}P_m^{-1}$.

To solve the problem Eq. (3), the time and the radial coordinate must be rescaled. For $P_m \gg 1$ the predominant term in Eq. (3) is the source term. Note that in the most part of the droplet the temperature increases uniformly, except in a thin zone near the surface of the droplet where the temperature increases rapidly (fig. 1-a). To follow this evolution of temperature in a range of very short time is necessary that $t \sim P_m^{-1}$ rescaled the scale time with $\tau = tP_m$.

To observe the variations of temperature in that very small region (interface liquid-gas or thermal boundary layer), we will perform the variable change $r = a - \varepsilon x$. It is worthy to mention that the appropriate length scale to observe the evolution of temperature is $\varepsilon \ll a$.

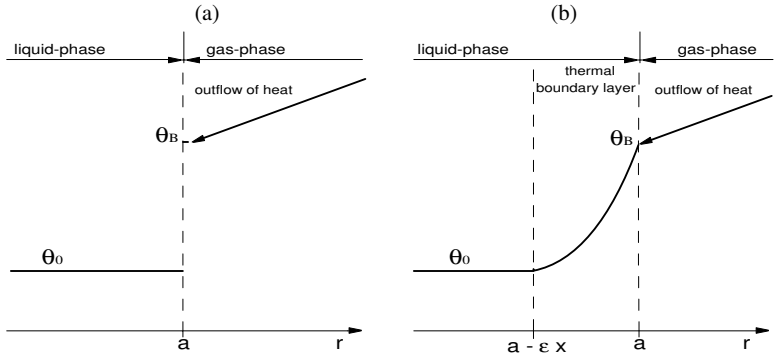

Figure 1. Temperature profile: (a) length scale $O(1)$. (b) lenght scale $O(\varepsilon)$

Equations (2) and (3) in the appropriate scale are written as:

$$\frac{d}{d\tau}(a^2) = -2\lambda \tag{5}$$

$$\frac{\partial\theta}{\partial\tau} - \frac{A}{\varepsilon^2}\frac{\partial^2\theta}{\partial x^2} = \frac{f^2\tau_m(\theta)}{1+(f\tau_m(\theta))^2}, \tag{6}$$

where $\lambda = \lambda^* P_m$, $\varepsilon \sim \sqrt{A/P_m}$. Note that, in these new variables the source term of Eq. (6) is the $O(1)$. An analysis of Eq. (6) for the condition $f \gg 1$ reveals that the source term behaves as $1/\tau_m(\theta)$ and for $f \ll 1$, it behaves as $f^2\tau_m(\theta)$. This work assumes that the energy dissipation is due to Brownian mechanism, whose relaxation time is inverse of the temperature $\tau_m(\theta) = 1/\theta$ [Maenosono and Saita, 2006]. Equation (6) is written as

$$\frac{\partial\theta}{\partial\tau} - \frac{\partial^2\theta}{\partial x^2} = \frac{f^2\theta}{\theta^2+f^2} \tag{7}$$

For the gas-phase a radial flow of vapor from the droplet to the ambient atmosphere is postulated. The equations governing the gas field surrounding of the droplet are presented below:

$$\epsilon\varrho P_m\frac{\partial\varrho}{\partial\tau} + \frac{1}{r^2}\frac{\partial}{\partial r}(r^2\varrho\nu) = 0$$

$$\epsilon\varrho P_m\frac{\partial y_i}{\partial\tau} + \varrho\nu\frac{\partial y_i}{\partial r} - \frac{1}{r^2}\frac{\partial}{\partial r}\left(\frac{r^2\theta^n}{L_i}\frac{\partial y_i}{\partial r}\right) = -s_i w_i, \quad i = O, F$$

$$\epsilon\varrho P_m\frac{\partial\theta}{\partial\tau} + \varrho\nu\frac{\partial\theta}{\partial r} - \frac{1}{r^2}\frac{\partial}{\partial r}\left(r^2\theta^n\frac{\partial\theta}{\partial r}\right) = Qw_F$$

Where $\epsilon = \rho_\infty/\rho_l$ (the subscript l represents liquid phase). Note that the time was rescaled with the order of magnitude of the liquid phase ($t \sim O(P_m^{-1})$). In this case, we consider that $\epsilon \ll 1$ (density of the liquid is much larger than the gas density) small enough such that $\epsilon P_m \ll 1$, the solution of the quasi-steady-state for the gas-phase may be allowed.

Now we have the gas conservation equations

$$r^2\varrho\nu = \lambda \tag{8}$$

$$\frac{\lambda}{r^2}\frac{\partial y_i}{\partial r} - \frac{1}{r^2}\frac{\partial}{\partial r}\left(\frac{r^2\theta^n}{L_i}\frac{\partial y_i}{\partial r}\right) = -s_i w_i, \quad i = O, F \tag{9}$$

$$\frac{\lambda}{r^2}\frac{\partial\theta}{\partial r} - \frac{1}{r^2}\frac{\partial}{\partial r}\left(r^2\theta^n\frac{\partial\theta}{\partial r}\right) = Qw_F \tag{10}$$

where L_i is the Lewis number of species i.

3. SOLUTION PROCEDURE

To solve the problem in liquid-gas interface it is necessary to match the solutions of the two phases with the following boundary conditions:

Inside the droplet, a region far from the surface results

$$\left(\frac{\partial\theta}{\partial r}\right)_{x\to\infty} = 0, \tag{11}$$

In the energy balance in the gas-liquid interface, it is assumed that part of the flow of heat from the hot environment is used to warm and partly to vaporize the droplet. As shown in the following relationship:

$$\left(x^2\theta^n\frac{\partial\theta}{\partial x}\right)_{x\to a^+} = \lambda\bar{L} + \left(\frac{k_l}{k_{g\infty}}x^2\frac{\partial\theta}{\partial x}\right)_{x\to a^-} = \lambda L_{\text{eff}} \tag{12}$$

where a^+ and a^- represent the droplet radius in the liquid phase and the droplet radius in the gas phase respectively, $\bar{L}$ the dimensionless latent heat of vaporization and L_{eff} is an effective heat of vaporization.

In the gas phase, one has

$$-\left(\frac{r^2\theta^n}{L_F}\frac{\partial y_F}{\partial x}\right) = \lambda(1-y_{Fs}), \quad \text{at} \quad x = a^+ \tag{13}$$

$$\theta = \theta_f, \quad \text{and} \quad y_F = y_O = 0 \quad \text{at} \quad r = r_f \tag{14}$$

$$\theta_\infty = y_{O_\infty} = 1 \quad \text{at} \quad r \to \infty \tag{15}$$

where the subscript f and ∞ represents the flame position and far from the droplet respectively.

The solution of Eqs. (8) to (10), with the boundary conditions (13) to (15) allowing to determine the rate of vaporization and the radius of the droplet as a function on the temperature on the surface of droplet. The mathematical development can be found any where [Fachini, 1999]. The effective heat of vaporization is described as

$$L_{\text{eff}} = \frac{Q + (1 - \theta_s - Q)[s/(s+1)]^{1/L_O}}{\{1 - \exp[\gamma(1 - \theta_B/\theta_s]\}^{-1/L_F} - [s/(s+1]^{1/L_O}}$$

where $Q = q/(c_p T_\infty)$ is the heat of combustion, θ_B the boiling temperature, θ_s surface temperature, $\gamma = L/(R_g T_B)$ (where L is the latent heat of vaporization, R_g is the universal gas constant, T_B is the boiling temperature dimensional), $s = \nu/Y_{o_\infty}$ (ν is the mass of oxidant burnt under stoichiometric conditions per unit of fuel mass, Y_{o_∞} is the mass fraction of oxygen in the ambient). The flame temperature as a function of surface temperature is described as

$$\theta_f = \theta_\infty + (\theta_s + Q - \theta_\infty - L_{\text{eff}})\left[1 - \left(\frac{s}{s+1}\right)^{1/L_O}\right]$$

and the rate of vaporization ($\lambda = \beta.a$) is obtained by the relation

$$\beta = \int_{\theta_s}^{\theta_f} \frac{\theta^n}{\theta - \theta_s + L_{\text{eff}}} d\theta + \int_{\theta_f}^{\theta_\infty} \frac{\theta^n}{\theta - \theta_s + L_{\text{eff}} - Q} d\theta$$

Once formulated the problem, Eqs. (5), (7), (11), (12), we are ready to solve numerically the liquid-phase problem by the finite difference method. One estimates an initial temperature at the droplet surface (below the boiling temperature) and with this temperature is obtained the properties in the gas-phase (latent heat effective, flame temperature, rate of vaporization, mass fraction of fuel on the surface of the droplet and the radius of the droplet). If the assigned temperature satisfies the condition at the interface, Eq. (12), we move to the next time step; otherwise, repeat the process until convergence.

4. RESULTS

This paper presents the results for the heating and vaporizing processes during the n-heptane droplet combustion, which is also heated by the magnetic nanoparticles, in the presence of an alternating magnetic field. The ambient temperature is the boiling temperature of fuel. For simplicity, we consider the Lewis number of fuel and oxidant be equal to unity. The properties of n-heptane are shown in the Table 1.

Table 1. Properties of fuel at 1 atm.

	T_B (K)	L (J/g)	q (J/g)	c_p $(J/g.K)$
n-heptane	371.15	316.76	44560.66	1.4

By increasing the frequency, the external magnetic field provides more energy for the droplets. And with this we will verify the influence of frequency on some properties as: the temperature profile within the droplet, the surface temperature of the droplet, the droplet radius, the square of the radius that in the classical solution is considered that this varies linearly with time, the rate of vaporization and the mass fraction of fuel at the droplet surface.

Because the source term is a function of f^2, where $f = 0.01$ and 100, already define the limits of variation with frequency. Therefore, we use frequencies in this interval.

In this work the problem was rescaled to verify the properties on the thermal boundary layer, inside of the droplet (outside the thermal boundary layer) the solution was already known [Fachini, 2009], Eq. (3) reduces to

$$\tau = (\theta^2 - \theta_0^2)/(2f^2) + \ln(\theta/\theta_0) \tag{16}$$

Equation (16) shows that for $f \ll 1$ (low frequency), $\theta = \theta_0$, and and this can be seen Fig.2, only within the thermal boundary layer the temperature increases, and this is due to the heat transfer from the gas-phase. In fig.3, where $f = 1$, can notice a strong influence on the heating of magnetic nanofluid. In this case the temperature evolution inside the droplet is written as $\tau = (\theta^2 - \theta_0^2)/2 + \ln(\theta/\theta_0)$.

For $f \gg 1$, the temperature is already strongly influenced by the alternating magnetic field, following $\theta = \theta_0 \exp(\tau)$, as can be seen in Fig.4.

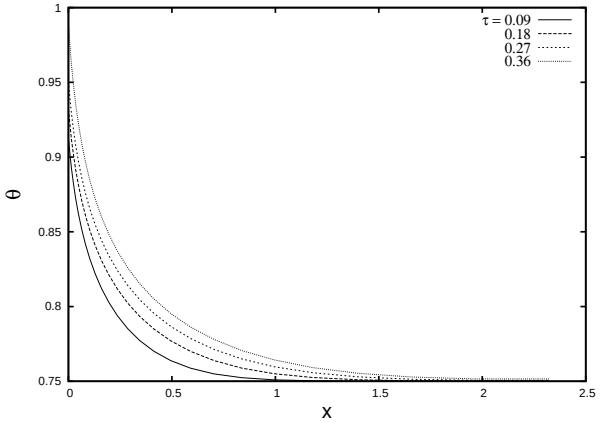

Figure 2. Profile of temperature for $f = 0.01$.

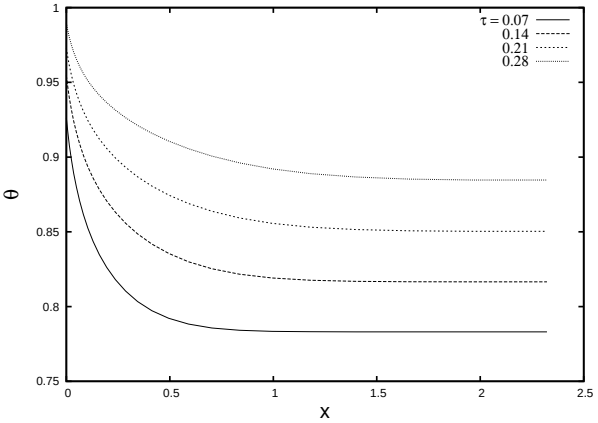

Figure 3. Profile of temperature for $f = 1$.

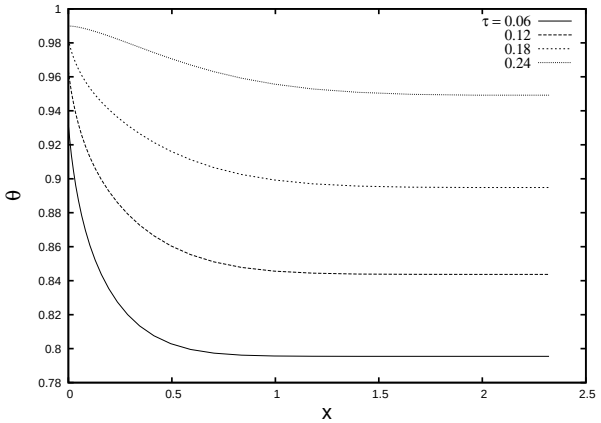

Figure 4. Profile of temperature for $f = 100$.

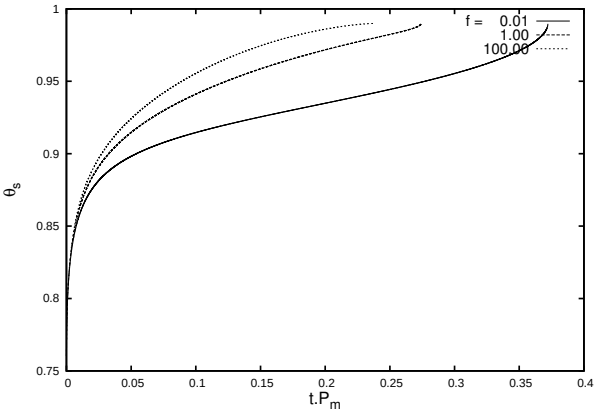

Figure 5. Surface temperature as a function of time.

Figure 5 shows the droplet surface temperature as a function of the time. It is expected that the surface temperature increases and remains almost constant when approaching the boiling temperature, but for $f = 1$ and 100, during a certain time the temperature rises quickly approaching the boiling temperature. This is explained by the fact that the boundary layer is valid only for times in which the condition $a \gg \varepsilon$ prevails.

As the droplet surface temperature reaching the boiling temperature more quickly with increasing of the frequency, the lifetime of the droplets decreases as shown in fig. 6. Remembering that in the classical model, the square of the radius (or diameter) decreases linearly with time (known as d^2 law)[Sirignano, 1999], but with the effect of external magnetic field in the magnetic nanofluid, the model does not describe this behavior because β changes with the time, as show the Fig. (7).

Figure 8, we can see that decreasing the lifetime of the droplet implies a higher rate of vaporization. The result shows that for a high frequency, the lifetime of the droplet is reduced approximately by 35%, consequently the mass fraction at droplet surface increases rapidly as as shown the Fig. 9, which was obtained by the Clausius-Clapeyron expression $y_{Fs} = \exp[\gamma(1 - \theta_B/\theta_s)]$, considering the vapor and liquid are in equilibrium at the interface liquid-gas [Fachini, 1999]. Note that significant vaporization occurs during the preheating droplet, that are the inicial instants where the graphics of Figs. 8 and 9 has the same behavior. Recalling that the first droplet is heated before of the evaporation, and this begins to evaporate long before reaching the boiling temperature.

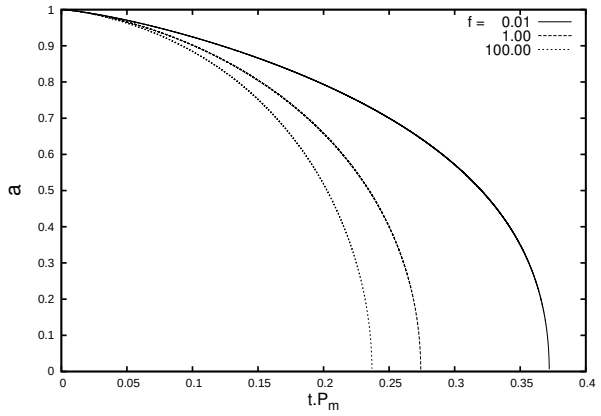

Figure 6. Radius as a function of time.

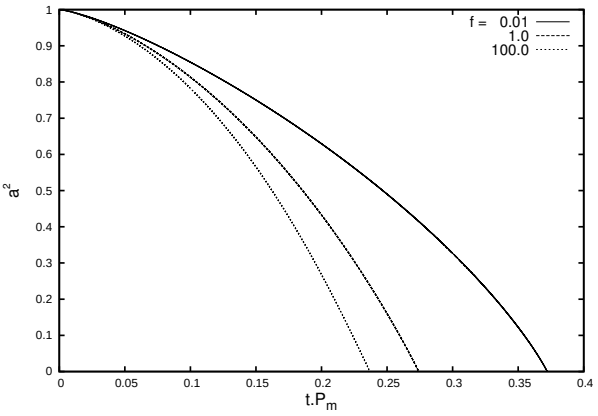

Figure 7. Square of the radius as a function of time

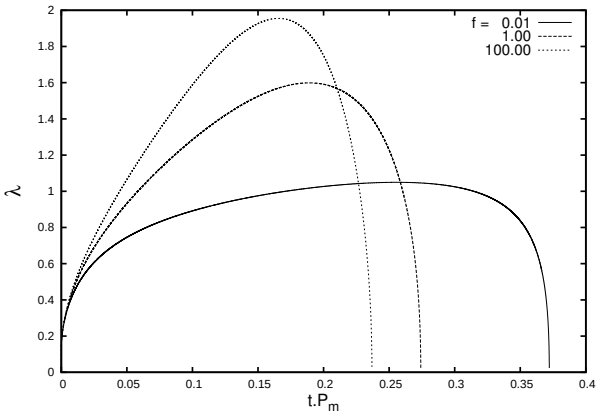

Figure 8. Vaporization rate as a function of time.

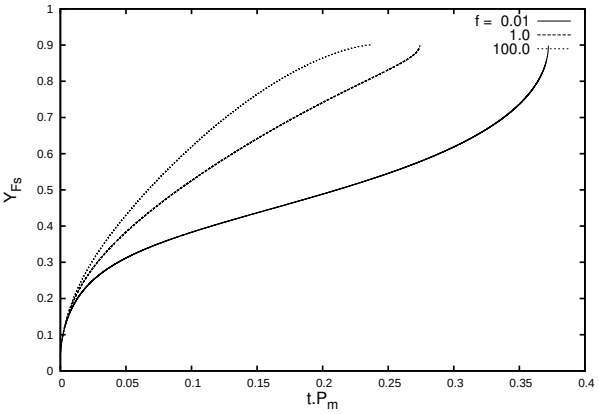

Figure 9. Mass fraction of fuel at the droplet surface as a function of time

5. CONCLUSION

In this work, the effect of the hyperthermia on the droplet heating and vaporization process is studied. It is observed that the magnetic energy source is responsible to heat the whole droplet and heat from the ambient is responsible to change the temperature profile only in a very thin layer close the surface. The combined heat sources are responsible to reduce the heating and vaporization times. Because there is substantially increasing of heating and vaporization rates, the magnetic field effect can be used to accelerate the vaporization, which will permit to construct short combustion chambers.

6. REFERENCES

Cristaldo, C. F. C., 2010, "Numerical solution for magnetic fluid droplet heating", Procedings of the VI National Congress of Mechanical Engineering, Campina Grande, PA, Brazil.

Fachini, F. F., 1999, "An analytical aolution for the quasi-steady droplet combustion", Combustion and Flame, 116, pp.

Fachini, F. F., 2009, "Heating of nanofluid droplet by high temperature ambient and magnetic field", Proceedings of the 20th International Congress of Mechanical Engineering, Gramado, RS, Brazil.

Kac, Mark, "Random Walk and the Theory of Brownian Motion", The American Mathematical Monthly, Vol. 54, No. 7, Part 1 (Aug. - Sep., 1947), pp. 369-391.

Maenosono, S., Saita, S., 2006, "Theoretical Assessment of FePt Nanoparticles as Heating Elements for Magnetic Hyperthermia", IEEE Transactions on Magnetic, vol. 42, pp. 1638-1642. 302-306.

Rosesweing, R.E., 2002, "Heating magnetic fluid with alternating field", Journal of Magnetism and Magnetic Materials, vol. 252, pp. 370-374.

Sirignano, W. A., 1999, "Fluid dynamics and transport of droplets and sprays", Cambrigde University Press.

Sthiech, G., 2003, "MOdelling engine spray and combustion processes" Hannover, Germany

Xuan,Y., Qiang Li, Meng ye, 2007, "Investigations of convective heat transfer in ferrofluid microflows using lattice-Boltzmann approach", International Journal of Thermal Sciences, Vol. 46, pp. 105-111.

7. Responsibility notice

The author(s) is (are) the only responsible for the printed material included in this paper